CO_2 Adsorption Hot Paper

Deutsche Ausgabe: DOI: 10.1002/ange.201600658
Internationale Ausgabe: DOI: 10.1002/anie.201600658

Selective CO_2 Adsorption in a Supramolecular Organic Framework

*Rahul S. Patil, Debasis Banerjee, Chen Zhang, Praveen K. Thallapally, and Jerry L. Atwood**

Abstract: *Considering the rapidly rising CO_2 level, there is a constant need for versatile materials which can selectively adsorb CO_2 at low cost. The quest for efficient sorptive materials is still on since the practical applications of conventional porous materials possess certain limitations. In that context, we designed, synthesized, and characterized two novel supramolecular organic frameworks based on C-pentylpyrogallol[4]arene (PgC_5) with spacer molecules, such as 4,4′-bipyridine (bpy). Highly optimized and symmetric intermolecular hydrogen-bonding interactions between the main building blocks and comparatively weak van der Waals interactions between solvent molecules and PgC_5 leads to the formation of robust extended frameworks, which withstand solvent evacuation from the crystal lattice. The evacuated framework shows excellent affinity for carbon dioxide over nitrogen and adsorbs ca. 3 wt % of CO_2 at ambient temperature and pressure.*

Civilization today is facing the greatest environmental concern in the form of rapidly rising level of CO_2 emission from anthropogenic sources.[1] Therefore, technologies that enable selective capture and sequestration of CO_2 from both immobile and mobile sources, such as thermal power plants and automobiles is of major importance.[2] The core of the technological innovations directed towards CO_2 capture and sequestration (CCS) is the development of next-generation CO_2 selective materials. Aqueous alkylamine solutions are currently used for CO_2 capture in power plants but have a severe energy penalty associated with regeneration of the amine solution.[3] Physisorption based CO_2 capture using solid-state porous materials, such as aluminosilicate zeolites,[4] activated carbon,[5] metal–organic Frameworks (MOFs),[6] and covalent organic frameworks (COFs)[7] stand as potential alternatives to liquid- or solvent-based capture techniques. MOF- and COF-based adsorbents are particularly interesting in terms of their chemical tenability, which allows pore surface modification with relative ease. Similarly, permanently porous supramolecular organic frameworks (SOFs) have been investigated for selective gas adsorption and separation.[8]

SOFs are the autonomous aggregations of two or more organic building components that are held together with non-covalent interactions, such as hydrogen bonds, halogen bonds, cation–π, π–π, and van der Waals forces. Shape and porosity of the SOFs are controlled through these non-covalent interactions. Most of the porous SOFs are crystallized with single component organic building blocks by varying different solvents, similar to preparing molecular crystals.[8b,9] The organic components within SOFs are closely packed to maximize the intermolecular interactions, and as a result the porosity in these crystals is often not spontaneous.[10] The attempt to generate porosity in such materials by means of solvent removal may result in the collapse of the entire molecular assembly into a densely packed or an amorphous phase.

However, careful selection of building blocks and meticulous engineering of the intermolecular interactions may afford a robust assembly which can withstand the removal of solvent molecules, forming a porous SOF. Herein, we report one such example of the design and synthesis of two novel SOFs based on multi-organic components and analyze their lattice stability upon solvent removal.

C-pentylpyrogallol[4]arene (PgC_5), 4,4′-bipyridine (bpy), and/or 1,2-bis(4-pyridyl)ethylene (bpe; Scheme 1) were selected as organic building blocks with acetonitrile (MeCN) as the solvent of crystallization. *C*-alkylpyrogallol-[4]arenes (PgCs) have proved to be excellent building blocks

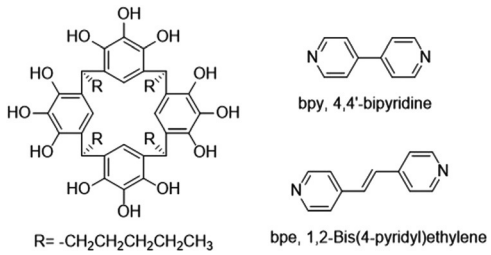

Scheme 1. Components of framework **1** and **2**.

for a variety of molecular architectures ranging from dimeric metal seamed capsules,[11] hexameric metal seamed capsules,[12] nanotubes,[13] nanocontainers,[14] to hydrogen-bonded hexamers.[15] All of these unique frameworks are held together by numerous thermodynamically stable intermolecular interactions within the respective systems. Similarly, both bpy and bpe are excellent hydrogen-bonding acceptors and thus can work as spacers in extended 3D hydrogen-bonded frameworks.[16] Recently, some of us showed that "a frustrated form" of PgC_5 has an affinity for CO_2 adsorption at high pressure.[17] Along the same line, we have attempted to enhance the CO_2 sorption ability of these PgC_5-based frame-

[*] R. S. Patil, Dr. C. Zhang, Prof. J. L. Atwood
Department of Chemistry
University of Missouri-Columbia
601 S College Ave, Columbia, MO 65211 (USA)
E-mail: AtwoodJ@missouri.edu
Dr. D. Banerjee, Dr. P. K. Thallapally
Fundamental and Computational Science Directorate
Pacific Northwest National Laboratory
Richland, WA 99352 (USA)
Supporting information and the ORCID identification number(s) for the author(s) of this article can be found under http://dx.doi.org/10.1002/anie.201600658.

works by co-crystallization of PgC_5 with organic spacer molecules under controlled conditions.

PgC_5 is synthesized using a previously reported acid-catalyzed condensation reaction of pyrogallol with hexanal in the presence of a small amount of conc. HCl.[18] The pure PgC_5 is recrystallized from hot acetonitrile solution and used for co-crystallization experiments. Equimolar solutions of PgC_5 and spacers (bpy/bpe) are prepared in acetonitrile and mixed in 1:2 v/v ratio. Single crystals of frameworks [(PgC_5)·2(bpy)·2(MeCN)] (**1**) and [(PgC_5)·2(bpe)·2(MeCN)] (**2**) were obtained by slow evaporation of the acetonitrile within 4–6 days.

Single-crystal X-ray diffraction (XRD) data reveals that the asymmetric unit of **1** contains one PgC_5, one bpy, and two acetonitrile molecules. The intermolecular interaction involves O-H···O (2.83 Å) hydrogen bonds (H-bonds) with two adjacent PgC_5 units which are slightly tilted with respect to the parent PgC_5 (Figure 1A). The parent PgC_5 forms O-H···O (2.78–2.98 Å) intermolecular H-bonding interactions with two adjacent inverted PgC_5. Two hydroxyl groups of the PgC_5 also form O-H···N (2.61–2.65 Å) interactions with two bpy molecules slightly tilted with respect to the PgC_5. Through the other end, these two bpy molecules also interact with two inverted PgC_5 units and form similar O-H···N interactions (Figure 1A). A solvent acetonitrile molecule also forms an O-H···N (2.84 Å) H-bond with one of the hydroxyl groups of the parent PgC_5.

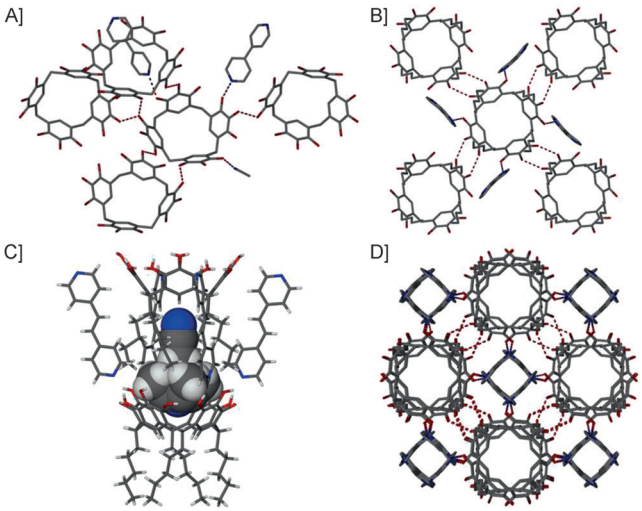

Figure 1. A) Intermolecular hydrogen-bonding pattern in **1** (*C*-pentyl tails of PgC_5 and hydrogen atoms are excluded for clarity). B) Intermolecular hydrogen-bonding pattern in framework **2** (hydrogen atoms are excluded for clarity). C) Acetonitrile molecules (space-filling model) occupying void spaces between head-to-tail arranged PgC_5. D) Extended view of hydrogen-bonding and stacked PgC_5 columns along the [001] crystallographic direction in **2** (hydrogen atoms are excluded for clarity). Dotted lines = hydrogen bonds. Red O, gray C, blue N, and white H.

The crystal structure of **2** shows the hydroxyl groups on the PgC_5 form four O-H···O (2.71 Å) intramolecular H-bonds and thus, maintains perfect cone/bowl shape geometry. The hydroxyl groups also interact with the hydroxyl groups of four inverted PgC_5 units forming a total of eight O-H···O (2.75 Å) intermolecular H-bonds (Figure 1B). These intermolecular interactions amongst PgC_5 molecules result in a wave-like H-bonding pattern between PgC_5. The parent PgC_5 also interact with four bpe molecules through O-H···N (2.68 Å) H-bonding interactions. Again, these four bpe molecules form O-H···N (2.68 Å) interactions with four inverted PgC_5, resulting in the formation of an extended wave-like H-bonding pattern between PgC_5 and bpe. In the extended crystal packing, all the PgC_5 are stacked head-to-tail on top of each other, thus forming columns of PgC_5 along the [001] crystallographic direction. Two disordered acetonitrile molecules occupy the void space between two head-to-tail arranged PgC_5 (Figure 1C). The slightly tilted bpe molecules are arranged in the space between four such columns of PgC_5. This extension of the framework along the [001] crystallographic direction affords the formation of small channels passing through the head-to-tail arranged PgC_5 columns (Figure 1D).

Since both frameworks possess distinct and unique arrangements of components in the crystal lattice, bulk synthesis of **1** (hereafter **B1**) and **2** (hereafter **B2**) were carried out. The experimental powder XRD patterns match well with the simulated powder XRD patterns from single-crystal data. In **B1**, out of two solvent acetonitrile molecules, one acetonitrile actually forms a hydrogen bond with the hydroxyl groups of the PgC_5. Thus, removing those solvent molecules resulted in the breaking down of the assembly. Whereas, in **B2** all hydroxyl groups of PgC_5 are bonded either with hydroxyl groups of other PgC_5 units or with bpe molecules.The solvent molecule is not directly hydrogen bonded to any other component of framework. Instead, it interacts with the bowl-shaped cavity and with the *C*-pentyl tail of the PgC_5 through comparatively weak van der Waals interactions. Thus, weakly bound acetonitrile molecules in **B2**, are comparatively easy to remove without breaking down the assembly. Thus, the remarkable thermal robustness of framework **B2** even at 120 °C is attributed to the evenly distributed hydrogen-bonding interactions and loosely bound solvent molecules. ^{1}H NMR spectroscopy and thermogravimetric analysis (TGA) of **B2** after heating at different temperatures confirm the loss of solvent molecules (Figure S8 and S13 in the Supporting Information). The single-crystal data of **2** (activated at 120 °C under dynamic vacuum for 12 h) shows no significant change in the arrangement of the PgC_5 and bpe. There is still some residual electron density attributable to the presence of partially occupied acetonitrile in the void spaces between the head-to-tail arranged PgC_5.

The permanently porous nature of **B2** was further confirmed by its gas adsorption ability. The sample was activated at 100 °C for 12 h under dynamic vacuum. Activated **B2** shows significantly higher CO_2 uptake (0.75 mmol g^{-1} at 298 K and 1 atm) compared to other gases, such as N_2, O_2, and Ar (Figure 2A). The amount of CO_2 adsorbed at 1 atm is 0.75 mole per mole of **B2**. The CO_2 uptake value is comparable to other SOF-based materials, such as SOF-1a, TBC[4]DHQ, and organic molecular cages, but lower than other classes of benchmark materials, such as MOFs, COFs, or aluminosilicate zeolites (Table 1). Moreover, the CO_2 adsorp-

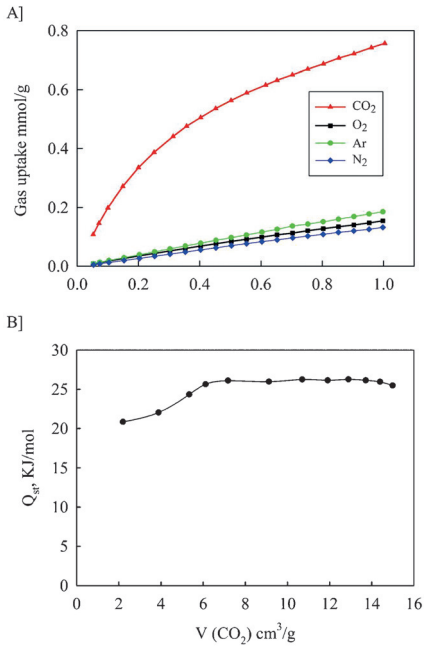

Figure 2. A) Adsorption isotherm of gases in **B2** at 298 K; B) Heat of Adsorption values of CO_2 adsorption in **B2**.

Table 1: CO_2 sorption data comparison.

Material[a]	V(CO_2) [$cm^3 g^{-1}$]	Q_{st} [KJ mol^{-1}][b]	Ref.
B2	15[a]	20	This work
SOF-1a	16a	27.6	[8b]
TPP	21[a]	–	[9b]
TBC[4]DHQ	35[b]	–	[8c]
Molecular cage	4.5[c]	–	[9a]

[a] CO_2 adsorption at 1 atm and 298 K. [b] CO_2 adsorption at 35 atm. [c] CO_2 adsorption at 1 atm and 293 K.

tion capacity of **B2** was found to be almost twenty times more than particular crystalline forms of parent PgC_5, under identical experimental conditions.[17] This result shows that the judicious choice of co-organic components can lead to multifold increase in the adsorption properties of a porous organic solid (PgC_5).

The heats of adsorption (Q_{st}) for CO_2 adsorption, calculated by fitting the adsorption data at 298 K and 288 K to the Clausius–Clapeyron equation, were found to be approximately 20 kJ mol^{-1} at zero loading (Figure 2B). We postulate that the adsorbed CO_2 molecules occupy the space vacated by acetonitrile molecules and thus interact with PgC_5 bowl-shaped cavity as well as the pyridine nitrogen atom of the bpe linker.[19] The shape similarity of the linear CO_2 molecules with acetonitrile also affords a significantly higher adsorption for CO_2 with respect to other adsorbate molecules. The difference in adsorption capacity of CO_2 and N_2 under ambient conditions highlights the potential of these materials for CO_2/N_2 separation from flue gas stream. To evaluate potential application of such materials for off-stream gas separation at high pressure, CO_2 and N_2 were introduced at 10 bar and 298 K. **B2** adsorbs 25 $cm^3 g^{-1}$ of CO_2 compared to 12 $cm^3 g^{-1}$ of N_2 at similar conditions. It is clear from adsorption curve that saturation capacity is not achieved yet and there is room for more CO_2 or N_2 to get inside (Figure S19 and S20).

In conclusion, herein we report a novel SOF material, synthesized by co-crystallization of an organic linker and a porous organic solid, showing multifold increase in gas-adsorption capacity with respect to each organic component. The strong CO_2 adsorption capacity of the SOF is related to interaction of the adsorbed CO_2 molecules with the pyridine nitrogen atom of the organic components. The high CO_2 selectivity of the SOF material over N_2 warrants further research on this type of material for gas adsorption and separation related application.

Experimental Section

Synthesis of frameworks:

[(PgC_5)·2(bpy)·2(MeCN)] (**1**): 2 ml of 0.01M *C*-pentylpyrogallol-[4]arene (PgC_5) in acetonitrile (MeCN) was mixed with 2 ml of 0.01M 4,4′-bipyridine (bpy) solution in the same solvent in a 20 mL glass vial. The clear solution was allowed to undergo slow solvent evaporation by unscrewing the lid of the vial. Colorless crystals were grown in the vial over 4–6 days.

[(PgC_5)·2(bpe)·2(MeCN)] (**2**): 2 ml of 0.01M PgC_5 in MeCN was mixed with 2 mL of 0.01M (1,2-bis(4-pyridyl)ethylene (bpe) solution in the same solvent in a 20 mL glass vial. The clear solution was allowed to undergo slow solvent evaporation by unscrewing the lid of the vial. Colorless crystals were grown in the vial over 3–4 days.

B1: 0.1 g of PgC_5 was mixed with 10 mL of acetonitrile at 80°C. To this hot clear solution, 0.037 g of bpy was added and stirred for 5 min at the same temperature. Heating of the reaction was turned off after 5 min. The white crystalline solid afforded thereafter is collected by filtration at room temperature and washed with 5 mL chilled acetonitrile and subsequently dried under vacuum at room temperature for 10 h. The purity of final product is (0.078 g, 56% yield) verified with ^{1}H NMR spectroscopy and powder X-ray diffraction.

B2: 0.1 g of PgC_5 was mixed with 10 mL of acetonitrile at 80°C. To this hot clear solution, 0.044 g of bpe is added and stirred for 5 min at the same temperature. Heating of the reaction was turned off after 5 min. The yellow crystalline solid afforded thereafter was collected by filtration at room temperature, washed with 5 mL chilled acetonitrile, and allow to dry under vacuum at room temperature for 10 h. The purity of product is (0.068 g, 47% yield) verified with ^{1}H NMR spectroscopy and powder X-ray diffraction.

CCDC 1445010, 1445011 and 1445012 contain the supplementary crystallographic data for this paper. These data can be obtained free of charge from The Cambridge Crystallographic Data Centre.

Full experimental details for the synthesis and characterization of the products and gas adsorption properties is available in the Supporting Information.

Keywords: CO_2 · gas sorption · hydrogen bonding · supramolecular organic frameworks · pyrogallol[4]arene

How to cite: *Angew. Chem. Int. Ed.* **2016**, *55*, 4523–4526
Angew. Chem. **2016**, *128*, 4599–4602

[1] V. A. Velazco, M. Buchwitz, H. Bovensmann, M. Reuter, O. Schneising, J. Heymann, T. Krings, K. Gerilowski, J. P. Burrows, *Atmos. Meas. Tech.* **2011**, *4*, 2809–2822.
[2] Z. Yuan, M. R. Eden, *Ind. Eng. Chem. Res.*, **2015**. Ahead of print. DOI: 10.1021/acs.iecr.5b03277..
[3] R. S. Haszeldine, *Science* **2009**, *325*, 1647–1652.

[4] a) K. Kusakabe, T. Kuroda, A. Murata, S. Morooka, *Ind. Eng. Chem. Res.* **1997**, *36*, 649 – 655; b) S. Cavenati, C. A. Grande, A. E. Rodrigues, *Chem. Eng. Sci.* **2006**, *61*, 3893 – 3906; c) S. Himeno, T. Tomita, K. Suzuki, S. Yoshida, *Microporous Mesoporous Mater.* **2007**, *98*, 62 – 69.
[5] a) C. F. Martín, M. G. Plaza, J. J. Pis, F. Rubiera, C. Pevida, T. A. Centeno, *Sep. Purif. Technol.* **2010**, *74*, 225 – 229; b) J. Silvestre-Albero, A. Wahby, A. Sepulveda-Escribano, M. Martinez-Escandell, K. Kaneko, F. Rodriguez-Reinoso, *Chem. Commun.* **2011**, *47*, 6840 – 6842.
[6] a) K. Sumida, D. L. Rogow, J. A. Mason, T. M. McDonald, E. D. Bloch, Z. R. Herm, T.-H. Bae, J. R. Long, *Chem. Rev.* **2012**, *112*, 724 – 781; b) J.-R. Li, R. J. Kuppler, H.-C. Zhou, *Chem. Soc. Rev.* **2009**, *38*, 1477 – 1504.
[7] a) L. Chen, P. S. Reiss, S. Y. Chong, D. Holden, K. E. Jelfs, T. Hasell, M. A. Little, A. Kewley, M. E. Briggs, A. Stephenson, K. M. Thomas, J. A. Armstrong, J. Bell, J. Busto, R. Noel, J. Liu, D. M. Strachan, P. K. Thallapally, A. I. Cooper, *Nat. Mater.* **2014**, *13*, 954 – 960; b) T. Mitra, K. E. Jelfs, M. Schmidtmann, A. Ahmed, S. Y. Chong, D. J. Adams, A. I. Cooper, *Nat. Chem.* **2013**, *5*, 276 – 281; c) R. Manurung, D. Holden, M. Miklitz, L. Chen, T. Hasell, S. Y. Chong, M. Haranczyk, A. I. Cooper, K. E. Jelfs, *J. Phys. Chem. C* **2015**, *119*, 22577 – 22586.
[8] a) J. Lü, C. Perez-Krap, M. Suyetin, N. H. Alsmail, Y. Yan, S. Yang, W. Lewis, E. Bichoutskaia, C. C. Tang, A. J. Blake, R. Cao, M. Schröder, *J. Am. Chem. Soc.* **2014**, *136*, 12828 – 12831; b) W. Yang, A. Greenaway, X. Lin, R. Matsuda, A. J. Blake, C. Wilson, W. Lewis, P. Hubberstey, S. Kitagawa, N. R. Champness, M. Schröder, *J. Am. Chem. Soc.* **2010**, *132*, 14457 – 14469; c) P. K. Thallapally, B. P. McGrail, J. L. Atwood, C. Gaeta, C. Tedesco, P. Neri, *Chem. Mater.* **2007**, *19*, 3355 – 3357.
[9] a) Y. Jin, B. A. Voss, R. D. Noble, W. Zhang, *Angew. Chem. Int. Ed.* **2010**, *49*, 6348 – 6351; *Angew. Chem.* **2010**, *122*, 6492 – 6495; b) P. Sozzani, S. Bracco, A. Comotti, L. Ferretti, R. Simonutti, *Angew. Chem. Int. Ed.* **2005**, *44*, 1816 – 1820; *Angew. Chem.* **2005**, *117*, 1850 – 1854.
[10] J. D. Dunitz, A. Gavezzotti, *Chem. Soc. Rev.* **2009**, *38*, 2622 – 2633.
[11] N. P. Power, S. J. Dalgarno, J. L. Atwood, *New J. Chem.* **2007**, *31*, 17 – 20.
[12] a) S. J. Dalgarno, N. P. Power, J. E. Warren, J. L. Atwood, *Chem. Commun.* **2008**, 1539 – 1541; b) J. L. Atwood, E. K. Brechin, S. J. Dalgarno, R. Inglis, L. F. Jones, A. Mossine, M. J. Paterson, N. P. Power, S. J. Teat, *Chem. Commun.* **2010**, *46*, 3484 – 3486.
[13] O. V. Kulikov, M. M. Daschbach, C. R. Yamnitz, N. Rath, G. W. Gokel, *Chem. Commun.* **2009**, 7497 – 7499.
[14] G. W. V. Cave, M. C. Ferrarelli, J. L. Atwood, *Chem. Commun.* **2005**, 2787 – 2789.
[15] a) S. J. Dalgarno, D. B. Bassil, S. A. Tucker, J. L. Atwood, *Angew. Chem. Int. Ed.* **2006**, *45*, 7019 – 7022; *Angew. Chem.* **2006**, *118*, 7177 – 7180; b) Q.-F. Zhang, R. D. Adams, D. Fenske, *J. Inclusion Phenom. Macrocyclic Chem.* **2005**, *53*, 275 – 279.
[16] a) R. S. Patil, H. Kumari, C. L. Barnes, J. L. Atwood, *Chem. Commun.* **2015**, *51*, 2304 – 2307; b) R. S. Patil, A. V. Mossine, H. Kumari, C. L. Barnes, J. L. Atwood, *Cryst. Growth Des.* **2014**, *14*, 5212 – 5218; c) R. S. Patil, H. Kumari, C. L. Barnes, J. L. Atwood, *Chem. Eur. J.* **2015**, *21*, 10431 – 10435.
[17] H. Kumari, L. Erra, A. C. Webb, P. Bhatt, C. L. Barnes, C. A. Deakyne, J. E. Adams, L. J. Barbour, J. L. Atwood, *J. Am. Chem. Soc.* **2013**, *135*, 16963 – 16967.
[18] F. Weinelt, H. J. Schneider, *J. Org. Chem.* **1991**, *56*, 5527 – 5535.
[19] R. Vaidhyanathan, S. S. Iremonger, G. K. H. Shimizu, P. G. Boyd, S. Alavi, T. K. Woo, *Science* **2010**, *330*, 650 – 653.

Received: January 20, 2016
Published online: March 1, 2016

